MODERN TRENDS IN PHYSICS RESEARCH

4th International Conference on Modern Trends in Physics Research

MTPR-10

Cairo University, Egypt 12 – 16 December 2010

EDITOR

Lotfia M. El Nadi

Cairo University, Egypt

CONFERENCE PROCEEDINGS ■ VOLUME 9910

World Scientific

NEW JERSEY • LONDON • SINGAPORE • BEIJING • SHANGHAI • HONG KONG • TAIPEI • CHENNAI

X-Rays of Heavy Elements for Nanotechnological Applications: W and Pb Ions

Sultana N. Nahar

Department of Astronomy, The Ohio State University, Columbus, OH 43210, USA
E-mail: nahar@astronomy.ohio-state.edu

Heavy elements can absorb or emit hard X-rays and hence are commonly implemented in various high energy nanotechnological applications. The absorptin or emission occurs mainly through the 1s-2p (K_α) transitions, and the process can be used as the source for production of radiation or electron in the applications. For enhanced productions of electrons and photons in the nanobiomedical applications, investigations have focused on the K-shell ionization of the atom or ion. This is because of the well-known rise in photoionization at the K-shell ionization threshold. However, experimental investigations to find any evidence of this rise has not been successful. We have developed a new method called *Resonant Theranostics* for biomedical applications, where we show that the energy for the rise is related to 1s-np, particularly to 1s-2p transitions which appear as resonances in the photoionization for heavy elements. The energy for the 1s-2p transitions varies some with the ionic state of the element and gives a narrow band resonant energy for the element. The strength of the process depends on the oscillator strength of the transitions. This report will demonstrate these through illustrations of the resonant energy range and strengths of photoabsorption due to K-alpha transitions using some elements, such as tungsten (W, Z=74) and lead (Pb, Z=82).
An X-ray photon can ionize a high-Z element by ejection of a K-shell electron. This will create a hole or vacancy which, through the Auger process, will be filled out by an upper shell electron with emission of a photon. Such process at the resonant energy can lead to Koster-Kronig cascade giving out a number of photons and electrons as the element goes through various ionic states and can be modeled using the oscillator strengths. Such emissions are highly desirable in radiation therapy application. Present illustrations will include electric dipole allowed transitions for nine ionic states, from hydrogen to fluorine like ions. The 2p subshell is filled beyond fluorine. The number of transitions in each ionic state is different because of different number of 2p electrons. There are 2, 2, 6, 2, 14, 35, 35, 14 and 2 transitions in H-, He-like, Li-like, Be-like, B-like, C-like, N-like, O-like, and F-like ions respectively, with a total of 112 Kα transitions for each element to occur in the event of breaking of the ionic states, such as, due to Auger process. The K_α transitions are found to be in hard X-ray region of 57 - 63 keV (0.22 - 0.20 Å) for W, and 71 - 80 keV (0.17 - 0.16 Å) for lead.

Keywords: Heavy element K_α transitions, Oscillator strengths; photoinization; Tungsten and Lead ions; Nanoparticles and Cancerous Tumors

1. Introduction

Heavy elements are of great interest in many areas, especially in biomedical and plasma applications. For example, gold nanoparticles are used in radiation therapy research. Gold is of particular interest since it is (i) non-reactive to body tissue, (ii) absorb hard X-rays that can have deeper tissue penetration, (iii) the X-rays are transparent to biogenic elements, such as, H, O, C, N, K, Fe. X-ray emissions from high-Z tungsten ions are useful for diagnostics of magnetically confined high temperature tokamak plasmas. Lead is one most known element for X-ray radiation shielding in biomedical, space and various other applications. However, detail study to understand the atomic properties of these ions has been very limited and hence the properties are largely unknown.

2. Auger Process and Resonant Theranostics

The present study on X-rays from heavy elements was initiated through a program that focuses on paradigm change from broad band to narrow band radiation for less harmful radiation therapy treatment. The new methodology *Resonant Theranostics* (RT)[?,?,?,1] proposes highly efficient treatment for cancerous tumors with use of high-Z nanoparticles. It employs resonant X-ray irradiation of the high-Z materials embeded in the tunor for potential usage as diagnostic and therapeutic (theranostics) agents. Research on mice has found that X-rays interaction with nanoparticles embedded in malignant tumors results in more effective treatment than that with direct irradiation.[?] X-rays interact more efficiently with high-Z elements in the nanoparticles leading to inner-shell ionization and producing Auger electrons and photons. These emissions could play an important role in destroying the surrounding malignant cells. RT predicts enhanced production of electrons at resonant energies and hence also seeks to create narrow band monochromatic radiation at the resonant energy which is described later.

The targeted monochromatic radiation should

CP 9910, Modern Trends in Physics Research
Fourth International Conference MTPR-10
edited by L. El Nadi

enhance absorption and be followed by emission of electrons and photons from inner shells via Auger process (Fig. 1). Ionization by X-ray photons (E_X) (> K-shell ionization energy E_K) can initiate the Auger process (Fig. 1(i)) where an inner shell electron vacancy is filled up by an upper shell electron which gives out excess energy by emitting a photon. This emitted photon can knock out another electron in the upper shell. The two newly created electron vacancies are filled up again by the higher orbital electrons with emission of two photons (Fig. 1(ii)). The process may continue to Coster-Kronig or Super-Coster-Kronig cascades until the holes have reached the outermost orbial.[?] Fig (iii) is the inverse of Auger where an 1s electron can be excited to upper vacancies in an external field. Resonant photo-excitation from 1s → 2p (with L-shell vacancy) can occur by an external monoenergetic X-ray source with an intensity above the predicted critical flux[?]

$$\Phi^c(\nu_{K\alpha}) = \frac{\sum_{n_i \geq 2} g_i A[n_i(S_i L_i J_i) \rightarrow 2(SLJ)]}{g_K B_{K\alpha}} \quad (1)$$

RT is based on the atomic properties of high-Z elements. However, these properties of heavy elements are largely unknown. Here we study the atomic transitions in W and Pb ions and predict the resonant energy range and strengths for enhanced emission of electrons and photons. K-shell ionization and K-shell transitions of both these elements occur at sufficiently high energies. We will illustrate that resonances are formed during X-ray interaction with the high-Z particle through inner shell, such as 1s-2p, transitions, and that these resonances represent higher absorption coefficients κ than at background, including that at the K-shell ionization energy, by orders of magnitude.

3. Atomic Processes and Parameters, and Theoretical Approach

Interaction between an atomic species X^{+z} of charge z and a X-ray photon usually lead to two processes, photo-excitation (inverse is de-excitation) and photoionization (inverse is electron-ion recombination). In photoexcitation an electron absorbs the photon and jumps to a higher excited level,

$$X^{+z} + h\nu \rightarrow X^{+z*}$$

but remains bound with the ion. The asterisk (*) denotes an excited state. Its strength is determined by the oscillator strength (f). The atomic parameter for de-excitation is the radiative decay rate or Einsteins A-coefficient. In photoionization/ photodissociation/ photo-electric effect an electron absorbs a photon and exits to continuum:

$$X^{+z} + h\nu \rightarrow X^{+z+1} + e$$

This direct ionization gives the background feature of the process. Photoionization can occur via an intermediate doubly excited autoionizing state as given below.

$$e + X^{+z} \rightleftharpoons (X^{+z-1})^{**} \rightleftharpoons \begin{cases} e + X^{+z} & \text{AI} \\ X^{+z-1} + h\nu & \text{DR} \end{cases}$$

The autoionizing state can lead either to autoionization (AI) when the electron goes free or dielectronic recombination (DR) when a photon is emitted. The inverse of DR is photoionization. The photoionization cross section is designated by σ_{PI}.

The atomic parameters are obtained from atomic structure calculations or the R-matrix method. In reletivistic Breit-Pauli approximation the Hamiltonian is written as (e.g.[?])

$$H^{\mathrm{BP}} = H^{NR} + H^{\mathrm{mass}} + H^{\mathrm{Dar}} + H^{\mathrm{so}} +$$

$$\frac{1}{2}\sum_{i \neq j}^{N}[g_{ij}(so + so') + g_{ij}(ss') + g_{ij}(css') +$$

$$g_{ij}(d) + g_{ij}(oo')] \quad (2)$$

where H_{NR} is the nonrelativistic Hamiltonian

$$H^{NR} = \sum_{i=1}^{N}\left\{-\nabla_i^2 - \frac{2Z}{r_i} + \sum_{j>i}^{N}\frac{2}{r_{ij}}\right\} \quad (3)$$

and relativistic one-body terms are, the mass correction $H^{mass} = -\frac{\alpha^2}{4}\sum_i p_i^4$, the Darwin term $H^{Dar} = \frac{\alpha^2}{4}\sum_i \nabla^2\left(\frac{Z}{r_i}\right)$, and the spin-orbit interaction $H^{so} = \left[\frac{Ze^2\hbar^2}{2m^2c^2r^3}\right]\mathbf{L}\,\mathbf{S}$. The rest of the terms are two-body terms where the Breit interaction is[?,?]

$$H^B = \sum_{i>j}[g_{ij}(so + so') + g_{ij}(ss')] \quad (4)$$

The Wave functions and energies are obtained solving $H\Psi = E\Psi$ where E < 0 for bound states. The transition matrix elements are obtained with dipole operator $\mathbf{D} = \sum_i \mathbf{r}_i$, where the sum is over all

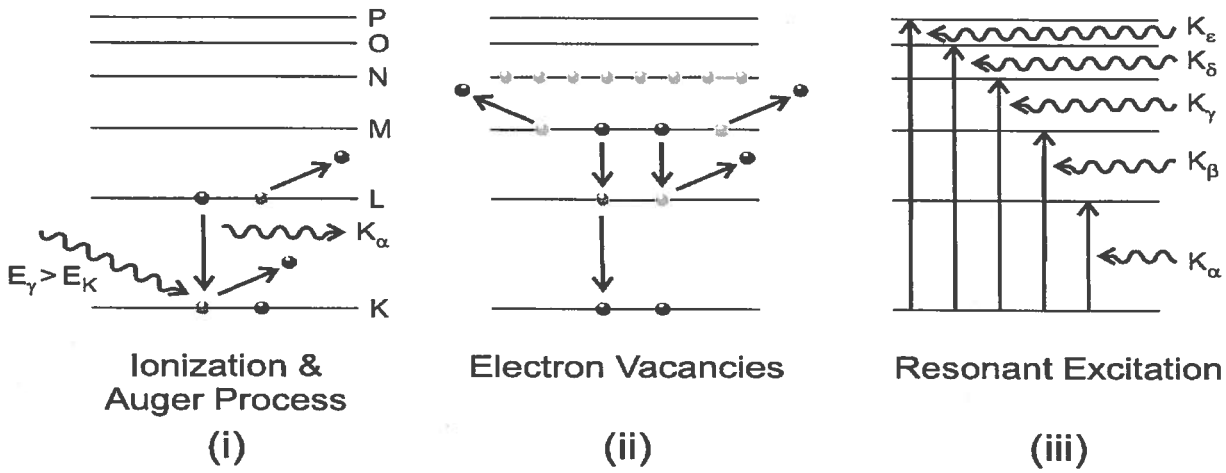

Fig. 1. i) Auger process, ii) Koster-Kronig cascade, iii) inverse of Auger process

electrons, which gives the generalized line strength as,

$$\mathbf{S} = \left| \left\langle \Psi_f \sum_{j=1}^{N} \mathbf{r_j} \Psi_i \right\rangle \right|^2 \tag{5}$$

The oscillator strength (f_{ij}), radiative decay rate (A_{ji}), photoionization cross section (σ_{PI}), and mass attenuation coefficient then can be expressed as follows

$$f_{ij} = \left[\frac{E_{ji}}{3g_i}\right] S \quad A_{ji}(sec^{-1}) = \left[0\ 8032 \times 10^{10} \frac{E_{ji}^3}{3g_j}\right] S$$

$$\sigma_{PI}(K\alpha\ \nu) = \frac{4\pi^2 a_o^2 \alpha}{3} \frac{E_{ij}}{g_k} S \quad \kappa(\nu; K\alpha) = \frac{\sigma_{PI}(\nu; K\alpha)}{uW_A} \tag{6}$$

where u is 1 amu=1.66054e-24 g and W_A is atomic weight.

The resonant structure in photoionization cross sections due to a K_α transition can be obtained by convolving the resonant cross sections over a normalized Gaussian function $\phi(\nu)$ as

$$\sigma_{PI}(K_\alpha)\phi(\nu) \quad \phi(\nu) = \frac{1}{\sqrt{2\pi}\Delta E} \exp\left[-\frac{E^2}{2\ \Delta E^2}\right] \tag{7}$$

4. Computations

The present energies and oscillator strengths for resonant 1s-2p transitions were obtained from configuration interaction atomic structure calculations using Thomas-Fermi approximation as implemented in the program SUPERSTRUCTURE (SS).[?,?] The 1s-2p transitions can occur for all ionic states of hydrogen like through fluorine like ions. States of each ion, such as, H-, He-, Li-, Be-, B-, C-, N-, O-, and F-like, were represented by a set of configurations as listed in Table 1. The sets are similar to those used earlier by Nahar et al[?] for gold ions. The later version of SS[?] which includes relativistic effects in Breit-Pauli approximations discussed above was used for the computations. Each set was optimized by inclusion of additional configurations and changing the values of the Thomas-Fermi parameters of the orbitals to obtain the lowest energies and correct order of states expected for these ions. Number of configurations and orbitals vary for each ions. The calculated f and A values were then processed to obtain other parameters using code PRCSS.[?]

5. X-ray Irradiation with Bremsstrahlung and Monochromatic Sources

In medical facilities, conventional machines use intense and high energy *broadband* X-rays in radiation therapy and diagnostics to ensure sufficient tissue penetration. The radiation is emitted as Bremsstrahlung radiation in the Roentgen X-ray tube which is very much the same as the original set-up. A beam of electrons is accelerated across the potential difference between the cathode and the anode, striking a high-Z target such as tungsten (Z=74), producing characteristic Bremsstrahlung radiation at all energies from zero to the peak value of

Table 1. Sets of configurations used in the atomic structure calculations for energies and oscillator strengths of K_α transitions in various ionic states, from H-like to F-like, of W and Pb. The configurations are numbered, within parentheses, for convenience of identification.

H-like
1s(1), 2s(2), 2p(3), 3s(4), 3p(5), 3d(6), 4s(7), 4p(8), 4d(9), 4f(10)
He-like
$1s^2$(1), 1s2s(2), 1s2p(3), 1s3s(4), 1s3p(5), 1s3d(6), 1s4s(7), 1s4p(8), 1s4d(9), 1s4f(10), $2s^2$(11), $2p^2$(12), $3s^2$(13), $3p^2$(14), $3d^2$(15), 2s2p(16), 2s3s(17), 2s3p(18), 2s3d(19), 2s4s(20), 2s4p(21), 2s4d(22), 2s4f(23), 2p3s(24), 2p3p(25), 2p3d(26), 2p4s(27), 2p4p(28)
Li-like
$1s^2$2s(1), $1s^2$2p(2), $1s^2$3s(3), $1s^2$3p(4), $1s^2$3d(5), $1s^2$4s(6), $1s^2$4p(7), $1s^2$4d(8), $1s^2$4f(9), 1s$2s^2$(10), 1s2s2p(11), 1s2s3s(12), 1s2s3p(13), 1s2s3d(14), 1s2s4s(15), 1s2s4p(16), 1s2s4d(17), 1s2s4f(18), 1s2p3s(19), 1s2p3p(20), 1s2p3d(21), 1s2p4s(22), 1s2p4p(23), 1s$2p^2$(24), 1s$3s^2$(25), 1s$3p^2$(26), 1s$3d^2$(27)
Be-like
$1s^2$$2s^2$(1), $1s^2$2s2p(2), $1s^2$$2p^2$(3), $1s^2$2s3s(4), $1s^2$2s3p(5), $1s^2$2s3d(6), $1s^2$2s4s(7), $1s^2$2s4p(8), $1s^2$2s4d(9), $1s^2$2s4f(10), $1s^2$2p3s(11), $1s^2$2p3p(12), $1s^2$2p3d(13), $1s^2$2p4s(14), $1s^2$2p4p(15), $1s^2$2p4d(16), $1s^2$2p4f(17), $1s^2$2s5s(18), $1s^2$2s5p(19), $1s^2$2s5d(20), $1s^2$2s5f(21), $1s^2$2s5g(22), $1s^2$2p5s(23), $1s^2$2p5p(24), $1s^2$2p5d(25), $1s^2$2p5f(26), $1s^2$2p5g(27), 1s$2s^2$2p(28), $1s^2$$3s^2$(29), $1s^2$$3p^2$(30), $1s^2$$3d^2$(31)
B-like
$1s^2$$2s^2$2p(1),$1s^2$2s$2p^2$(2), $1s^2$$2p^3$(3), $1s^2$$2s^2$3s(4), $1s^2$$2s^2$3p(5), $1s^2$$2s^2$3d(6), $1s^2$2s2p3s(7), $1s^2$2s2p3p(8), $1s^2$2s2p3d(9), $1s^2$$2s^2$4s(10), $1s^2$$2s^2$4p(11), $1s^2$$2s^2$4d(12), $1s^2$$2s^2$4f(13), $1s^2$2s2p4s(14), $1s^2$2s2p4p(15), $1s^2$2s2p4d(16), $1s^2$2s$3d^2$(17), $1s^2$$2p^2$3s(18), $1s^2$$2p^2$3p(19), $1s^2$$2p^2$3d(20), $1s^2$$2p^2$4s(21), $1s^2$$2p^2$4p(22), 1s$2s^2$$2p^2$(23), 1s$2s^2$2p3p(24), 1s$2s^2$2p3d(25)
C-like
$1s^2$$2s^2$$2p^2$(1), $1s^2$2s$2p^3$(2), $1s^2$$2p^4$(3), $1s^2$$2s^2$2p3s(4), $1s^2$$2s^2$2p3p(5), $1s^2$$2s^2$2p3d(6), $1s^2$$2s^2$2p4s(7), $1s^2$$2s^2$2p4p(8), $1s^2$$2s^2$2p4d(9), $1s^2$$2s^2$2p4f(10), $1s^2$2s$2p^2$3s(11), $1s^2$2s$2p^2$3p(12), $1s^2$2s$2p^2$3d(13), $1s^2$2s$2p^2$4s(14), $1s^2$2s$2p^2$4p(15), $1s^2$2s$2p^2$4d(16), 1s$2s^2$$2p^3$(17)
N-like
$1s^2$$2s^2$$2p^3$(1), $1s^2$2s$2p^4$(2), $1s^2$$2s^2$$2p^2$3s(3), $1s^2$$2s^2$$2p^2$3p(4), $1s^2$$2s^2$$2p^2$3d(5), $1s^2$$2s^2$$2p^2$4s(6), $1s^2$$2s^2$$2p^2$4p(7), $1s^2$$2s^2$$2p^2$4d(8), $1s^2$$2s^2$$2p^2$4f(9), $1s^2$$2p^5$(10), $1s^2$2s$2p^3$3s(11), $1s^2$2s$2p^3$3p(12), $1s^2$2s$2p^3$3d(13), 1s$2s^2$$2p^4$(14)
O-like
$1s^2$$2s^2$$2p^4$(1), $1s^2$2s$2p^5$(2), $1s^2$$2p^6$(3), $1s^2$$2s^2$$2p^3$3s(4), $1s^2$$2s^2$$2p^3$3p(5), $1s^2$$2s^2$$2p^3$3d(6), $1s^2$$2s^2$$2p^3$4s(7), $1s^2$$2s^2$$2p^3$4p(8), $1s^2$$2s^2$$2p^3$4d(9), $1s^2$$2s^2$$2p^3$4f(10), $1s^2$2s$2p^4$3s(11), $1s^2$2s$2p^4$3p(12), $1s^2$2s$2p^4$3d(13), $1s^2$2s$2p^4$4s(14), $1s^2$2s$2p^4$4p(15), $1s^2$2s$2p^4$4d(16), $1s^2$$2s^2$$2p^2$$3s^2$(17), 1s$2s^2$$2p^5$(18)
F-like
$1s^2$$2s^2$$2p^5$(1), $1s^2$2s$2p^6$(2), $1s^2$$2s^2$$2p^4$3s(3), $1s^2$$2s^2$$2p^4$3p(4), $1s^2$$2s^2$$2p^4$3d(5), $1s^2$$2s^2$$2p^4$4s(6), $1s^2$$2s^2$$2p^4$4p(7), $1s^2$$2s^2$$2p^4$4d(8), $1s^2$$2s^2$$2p^4$4f(9), $1s^2$2s$2p^5$3s(10), $1s^2$2s$2p^5$3p(11), $1s^2$2s$2p^5$3d(12), $1s^2$2s$2p^5$4s(13), $1s^2$2s$2p^5$4p(14), $1s^2$2s$2p^5$4d(15), 1s$2s^2$$2p^6$(16)

the potential denoted as KVp (peak voltage). X-ray sources are typically two types, one up to 100-250 kVp, and the other, employing linear accelerators, up to about 10-15 MVp. Exposure to wide wavelength Bremstruhlung is not necessary for the treatment, rather harmful to body tissue, as shown in Fig. 2. While the low energy X-rays below few tens of KeV are absorbed by the tissue without any significant penetration, high energy radiation passes through without significant attenuation. Therefore, for both the low energy and the high energy X-ray sources it becomes necessary to increase radiation dosage to high levels for diagnostics (imaging) or, even more so, for therapy.

To avoid collateral damage Resonant Theranostics[?,?,?] aims to generate and employ *monochromatic* or narrow band radiation that spectroscopically correspond to resonant transitions of the nanoparticles doped in the tumor as shown in Fig. 3.

The advantage of monochromatic over Bremsstrahlung radiation is that we may control and target specific features in X-ray photoionization cross sections for maximal radiation absorption. Such spectroscopic radiation should be far more efficient with reduced exposure. In addition, in contrast to broadband imaging, spectroscopy gives more detailed microscopic and accurate information. One particular technique to generate the targeted radia-

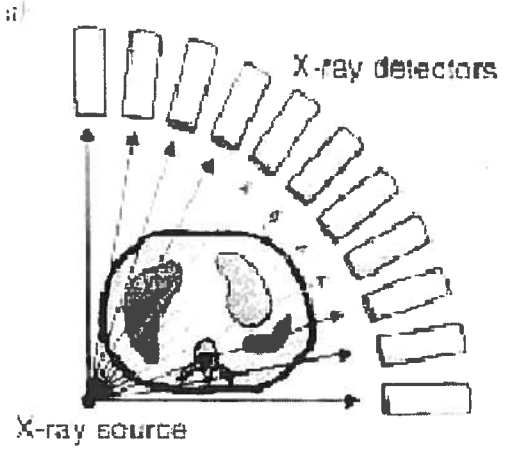

Fig. 2. Over exposure of radiation in conventional radiation therapy

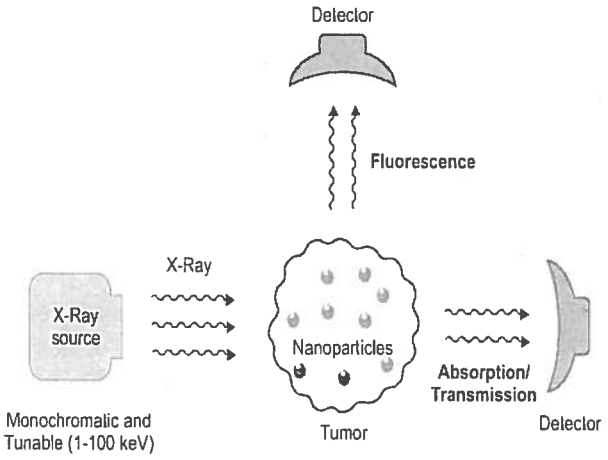

Fig. 3. Experimental set-up of RT.[?] At resonant energies, fluorescent emission and electrons due to inner-shell ionization following brief impact will breakup the DNA or destroy tumor cells locally.

tion is based on partial conversion of Bremsstahlung radiation into monochromatic Kα energy according to the following expression

$$I(K\alpha) \propto N(X) \int_{E \geq E_K}^{E=E(kVp)} f_B(E)\sigma_K(E)dE \quad (8)$$

where N(X) is number density of atoms of element X, f_B is the Bremsstahlung flux from an ordinary X-ray source, and σ_K is the K-shell photoionization cross section. It may be assumed, to a good approximation, that each K-shell ionization leads to the production of a K_α photon. The K-fluorescence yield may be expressed as

$$\omega_K = \frac{A_r(L-K)}{A_r(L-K) + A_a(L)} \quad (9)$$

where A_r and A_a are the radiative and autoionization decay rates respectively. It follows that all photons from the Bremsstrahlung source above the K-shell ionization energy, with E > E_K, may be *converted* into monochromatic K_α radiation with high efficiency. Moreover, such monochromatic deposition of X-ray energy may be localized using high-Z material, such as nanoparticles, embedded in cancerous tumors.[?] Monte Carlo simulations using the Geant4 computational package have shown[?] that the RT scheme would enhance the rate of Auger processes via Coster-Kronig and Super-Coster-Kronig branching transitions,[?] and result in significant production of electron ejections and photon emission.

6. Results and Discussion

We present atomic parameters for all possible allowed E1 fine structure transitions $1s^p - 2p^q$, where $p \leq 2$ and $q \leq 6$ of W and Pb ions, in the following subsection. The resonances corresponding to these transitions in photoionization, and attenuation coefficients relevant to biomedical applications, are discussed in the next subsection.

6.1. *1s-2p K_α Transitions of W and Pb ions*

Oscillator strength (f_{ij}), line strength (S), radiative decay rate A_{ji} in sec^{-1}, and the corresponding cross section (σ_{PI}) for various resonant K_α transitions for all ionic states, from hydrogen to fluorine like, of tunsten and lead are presented in Table 2. The table gives the symmetries (slp) with configuration numbers (ci and cj), the transition wavelength (wl)in Å and the energy E in KeV and individual level energies E_i and E_j in Ry of transitional levels i and j. The numbers within parentheses of the transitional configurations C_i and C_j corresponds to configuration numbers, that is, their positions in the set of configurations used in the calculations (Table 1). For an estimation of average stregnth of the transitions, the LS multiplet values calculated from transitions of same-spin multiplicity are also given. The last line includes the total oscillator strength, cross section (Megabarns), and absorption coefficient in cm^2/g.

The number of 1s-2p or K_α transitions varies from 2 to 35 due to different number of electrons in 2p subshell as the possible number of states formation changes with them. There are 2, 2, 6, 2, 14, 35, 35, 14 and 2 K_α transitions in H-like, He-like, Li-like, Be-like, B-like, C-like, N-like, O-like, and F-like ions respectively. These include both types of electric dipole (E1) allowed transitions, same-spin multiplicity and intercombination. Hence, in case of ionic breakdown due to cascades of electron droppings and ejections initiated by an Auger process, a total sum of 112 K_α transitions are possible to occur. Both tungsten and lead ions have K_α lines in the hard X-rays. They are in the energy region of 57 - 63 keV (0.22 - 0.20 $\AA$) for tunsten ions and 71 - 80 keV (0.17 - 0.16 $\AA$) for lead ions.

To the best of our knowledge these are the first calculations for the K_α transitions of these elements and ions. While experimental data are available for ionization edges of elements, excitation data are rare. As such it is not possible to compare with existing values. For all ionic states, the states of the ground configuration are found to be in the expected right order, except the nitrogen like ions. The expected order of states of the ground configuration of a nitrogen-like ion is $2s^2 2p^3(^4S^o)$, $2s^2 2p^3(^2D^o)$, and $2s^2 2p^3(^2P^o)$. The present computation using SS[7] yields the right order in LS coupling. However, relativistic Breit-Pauli calculations for fine structure shifts the levels such that $2s^2 2p^3(^2D^o_{3\ 2})$ lies lower than the level $2s^2 2p^3(^4S^o_{3\ 2})$. We expect N-like configuration to be more sensitive to relativistic effects, since it has a half-filled subshell, compared to other ions. Hence not only relativistic effects, but also more electron correlation are more sensitive than for other ions with lesser number of active electrons in the 2p-subshell. The Breit-Pauli Hamiltonian (Eq. 1) implies that both the relativistic and electron correlation effects are important in determining the energies and transition probabilities. But while higher order Breit-Pauli corrections may play a role, it is unlikely that the order of levels would change from what is obtained at lower Z, such as for N-like iron and other similar ions. Since no other experimental or calculated values are avaialble, it is difficult to determine the exact accuracy in the present results.

We expect that, with the exception of N-like W and Pb, our results should be accurate to 5-15% for energies, and 10-30% for radiative transition probabilities of strong E1 transitions. However, we note that there are 112 K-alpha transitions and many of them are exceedingly weak. For those transitions the uncertainty in transition probabilities would likely be much higher, perhaps a factor of two or more. The main purpose of the present work is to obtain reasonably accurate values and line strengths to indicate approximate positions of $K\alpha$ resonance complexes that may potentially participate in Auger processes upon X-ray irradiation.

6.2. *Energies and Strengths in Resonant X-ray Photoionization*

The excitation energies of 1s into the 2p lie above the ionization limit of both W and Pb. Hence the 1s-2p transition arrays from H-like to F-like ionization states of these ions correspond to autoionizing resonances and appear as resonances in photoionization cross sections. The background photoionizaton cross section (σ_{PI}) without any autoionizing resonances decreases monotonically with photon energy. As the energy reaches the ionization energy of an inner orbital or shell, the cross section shows a jump at the energy, beyond which it decreases until the energy reaches to the next threshold energy of a deeper inner shell.

The curves in Figs 1 and 2 are the background mass absorption coefficient ($\kappa = \sigma_{PI}\ m$) of neutral W and Pb.[7] The background structure of κ is the same as that of σ_{PI} except the constant factor of mass 1 m. The rises Figs. 1 and 2 correspond to enhancements in κ at ionization thresholds of electronic shells K, L and M (pointed out by arrows). The rise at K-shell ionization energy E_K, ~70 keV for W and ~88 keV for lead, are 10.8 cm^2/g and 7.32 cm^2/g respectively, much smaller in magnitude compared to the low energy cross sections. E_K has been the focus of experiments but without success to see the rise. The reason is the low magnitude of the K-shell ionization rise and hence lower probability for ionization.

The enhanced emission of electrons can occur through the autoionizing resonances due to 1s-2p transitions. The figures show the these resonances in all hydrogen to fluorine ionic states lying below the K-shell ionization edge for W and Pb in the energy ranges 57 - 63 keV and 71 - 80 keV respectively. It is clear that the peaks of these resonances are far higher, differing by orders of magnitude, than the

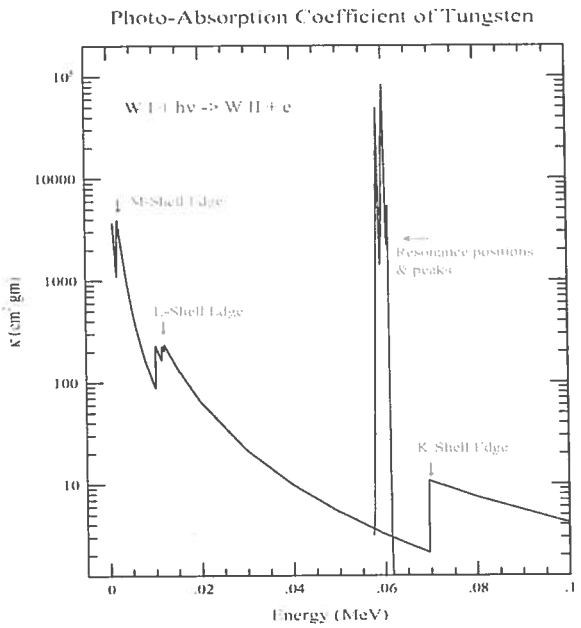

Fig. 4. Absorption coefficient κ of tunsten (W). Various rises correspond to enhancements in ionization at K, L, M (sub)-shells energies: E_K, E_L, E_M. The predicted K_α resonant structure in the energy range of 0.057 - 0.063 MeV is orders of magnitude higher that that at K-shell ionization edge.

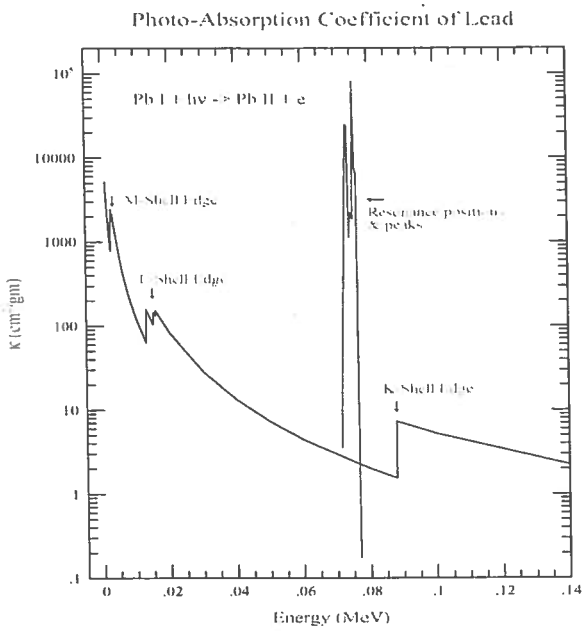

Fig. 5. Absorption coefficient κ of lead (Pb). Various rises correspond to enhancements in ionization at K, L, M (sub)-shells energies: E_K, E_L, E_M. The predicted K_α resonant structure in the energy range of 0.071 - 0.080 MeV is orders of magnitude higher that that at K-shell ionization edge.

jump at the K-shell edge. The physical consequence is that the X-ray photoabsorption probability over the spread of the k_α resonances is considerably higher than at the K-shell ionization edge. Such an absorption of radiation should lead to Auger processes, and possible cascade of Coster-Kronig and Super-Coster-Kronig transitions, resulting in enhanced emission of electrons and photons.

7. Conclusion

Energies and transition strengths of K_α transitions are presented for all ionic states from hydrogen to fluorine-like of two high-Z elements W and Pb. The transition strengths have been converted into cross sections to illustrate that these represent strong resonances with much higher probability of ionization than at the K-shell ionization threshold. Hence these resonant energies could be the focus for potential biomedical applications using monochromatic X-ray sources.

8. Acknowledgment

Partially supported by DOE-NNSA and NASA. Computations were carried out at the Ohio Supercomputer Center.

References

1. A.K. Pradhan *et al.*, *The Radiotherapy Dynamics (XVth Int. Conf. Use of Comput. in Radiat. Ther.) Vol.* **2**, 89 (2007)
2. E. Silver, A.K. Pradhan,Y. Yu, *RT Image* **21**, 30 (2008)
3. A.K. Pradhan, S.N. Nahar, M. Montenegro *et al.*, *J. Phys. Chem.* A **113**, 12356 (2009)
4. M. Montenegro, S.N. Nahar, A.K. Pradhan *et al.*, *J. Phys. Chem.* A **113**, 12364 (2009)
5. J. Hainfeld *et al.*, *Phys. Med. Biol.* **49**, N309 (2004)
6. Anil K. Pradhan and Sultana N. Nahar, *Atomic Astrophysics and Spectroscopy* (Cambridge University Press, 2011).
7. S.N. Nahar, W. Eissner, G.X. Chen, A.K. Pradhan, *Astronomy & Astrophys.* **408**, 789 (2003)
8. S.N. Nahar, *Astron. Astrophys* **448**, 779 (2006)
9. W. Eissner, M. Jones, H. Nussbaumer, *Comput. Phys. Commun.* **8**, 270 (1974)
10. S.N. Nahar, A.K. Pradhan, C. Sur, *J. Quant. Spec. Rad. Transfer* **109**, 1951 (2008)
11. NIST website: http://physics.nist.gov/PhysRefData/Xcom

Table 2. Oscillator strength (f_{ij}), line strengths (S), radiative decay rate (A_{ji}), and cross section σ_{PI} for 1s-2p K_α transitions in W and Pb ions.

Z	Ne	slpc:i	slpc:j	gi	gj	wl(Å)	E(Kev)	Ei(Ry)	Ej(Ry)	fij	S	Aji(s-1)	σ_{PI}(Mb)
W Ions													
H-like: C_i(1)=1s , C_j(3)= 2p													
74	1	2Se 1	2Po 3	2	2	0.208	59.608	0.00	4390.69	1.03E-01	1.41E-04	1.60E+16	8.34E-01
74	1	2Se 1	2Po 3	2	4	0.203	61.076	0.00	4497.81	2.03E-01	2.71E-04	1.65E+16	1.64E+00
LS						4462.10	60.710	0.00	4462.10	3.07E-01	4.13E-04	1.64E+16	2.48E+00
Total:No of trans= 2						Ekev= 60.710		f,CS,Absrp cf=			3.07E-01	2.47E+00	8.11E+03
He-like: C_i(1)=1s1s , C_j(3)= 1s2p													
74	2	1Se 1	1Po 3	1	3	0.206	60.187	0.00	4433.95	4.14E-01	2.80E-04	2.18E+16	3.34E+00
74	2	1Se 1	3Po 3	1	3	0.21	58.760	0.00	4328.91	1.92E-01	1.33E-04	9.64E+15	1.55E+00
LS						4433.95	60.327	0.00	4433.95	4.14E-01	2.80E-04	2.18E+16	3.34E+00
Total:No of trans= 2						Ekev= 60.327		f,CS,Absrp cf=			6.06E-01	4.89E+00	1.60E+04
Li-like: C_i(1)=1s1s2s , C_j(11)= 1s2s2p													
74	3	2Se 1	2Po11	2	2	0.209	59.323	0.00	4358.21	5.33E-02	7.34E-05	8.13E+15	4.30E-01
74	3	2Se 1	2Po11	2	4	0.206	60.187	0.00	4427.22	1.91E-01	2.58E-04	1.50E+16	1.54E+00
74	3	2Se 1	2Po11	2	2	0.206	60.187	0.00	4430.65	1.30E-01	1.75E-04	2.04E+16	1.04E+00
74	3	2Se 1	2Po11	2	4	0.204	60.777	0.00	4458.68	8.48E-02	1.14E-04	6.77E+15	6.84E-01
74	3	2Se 1	4Po11	2	2	0.21	58.760	0.00	4321.92	1.46E-02	2.03E-05	2.20E+15	1.18E-01
74	3	2Se 1	4Po11	2	4	0.21	58.760	0.00	4325.32	1.20E-01	1.66E-04	8.98E+15	9.64E-01
LS						4426.77	60.229	0.00	4426.77	4.58E-01	6.21E-04	2.40E+16	3.70E+00
Total:No of trans= 6						Ekev= 60.229		f,CS,Absrp cf=			5.92E-01	4.78E+00	1.56E+04
Be-like: C_i(1)=1s1s2s2s , C_j(28)= 1s2s2s2p													
74	4	1Se 1	1Po28	1	3	0.206	60.187	0.00	4429.21	3.63E-01	2.46E-04	1.91E+16	2.93E+00
74	4	1Se 1	3Po28	1	3	0.21	59.040	0.00	4336.76	1.69E-01	1.17E-04	8.50E+15	1.36E+00
LS						4429.21	60.263	0.00	4429.21	3.63E-01	2.46E-04	1.91E+16	2.93E+00
Total:No of trans= 2						Ekev= 60.263		f,CS,Absrp cf=			5.32E-01	4.29E+00	1.40E+04
B-like: C_i(1)=1s1s2s2s2p , C_j(22)= 1s2s2s2p2p													
74	5	2Po 1	2De22	2	4	0.206	60.187	0.00	4416.09	4.91E-04	6.67E-07	3.84E+13	3.96E-03
74	5	2Po 1	2De22	4	4	0.211	58.760	95.73	4416.09	1.96E-02	5.45E-05	2.94E+15	1.58E-01
74	5	2Po 1	2De22	4	6	0.211	58.760	95.73	4418.99	9.54E-02	2.65E-04	9.55E+15	7.69E-01
74	5	2Po 1	2Pe22	2	2	0.206	60.187	0.00	4419.97	1.30E-01	1.76E-04	2.04E+16	1.05E+00
74	5	2Po 1	2Pe22	4	2	0.211	58.760	95.73	4419.97	3.18E-02	8.82E-05	9.55E+15	2.56E-01
74	5	2Po 1	2Pe22	2	4	0.202	61.378	0.00	4515.88	1.71E-05	2.28E-08	1.40E+12	1.38E-04
74	5	2Po 1	2Pe22	4	4	0.206	60.187	95.73	4515.88	1.87E-01	5.08E-04	2.94E+16	1.51E+00
74	5	2Po 1	2Se22	2	2	0.202	61.378	0.00	4517.82	1.30E-05	1.73E-08	2.13E+12	1.05E-04
74	5	2Po 1	2Se22	4	2	0.206	60.187	95.73	4517.82	4.59E-02	1.25E-04	1.44E+16	3.70E-01
74	5	2Po 1	4Pe22	2	2	0.21	58.760	0.00	4325.37	8.88E-02	1.23E-04	1.34E+16	7.16E-01
74	5	2Po 1	4Pe22	4	2	0.21	57.667	95.73	4325.37	6.73E-05	1.91E-07	1.93E+13	5.42E-04
74	5	2Po 1	4Pe22	2	4	0.21	60.187	0.00	4421.30	2.46E-01	3.34E-04	1.93E+16	1.98E+00
74	5	2Po 1	4Pe22	4	4	0.21	58.760	95.73	4421.30	4.30E-02	1.19E-04	6.46E+15	3.47E-01
74	5	2Po 1	4Pe22	4	6	0.21	60.187	95.73	4512.22	4.93E-02	1.34E-04	5.15E+15	3.97E-01
LS						4388.98	59.715	68.38	4457.36	2.97E-01	1.22E-03	2.75E+16	2.39E+00
Total:No of trans= 14						Ekev= 59.715		f,CS,Absrp cf=			9.37E-01	7.56E+00	2.48E+04
C-like: C_i(1)=1s1s2s2s2p2p , C_j(17)= 1s2s2s2p2p2p													
74	6	3Pe 1	3Po17	3	5	0.210	59.040	94.20	4424.11	6.98E-02	1.45E-04	6.31E+15	5.63E-01
74	6	3Pe 1	3Po17	5	5	0.215	57.667	191.83	4424.11	2.67E-05	9.46E-08	3.84E+12	2.15E-04
74	6	3Pe 1	3Po17	1	3	0.206	60.187	0.00	4427.07	3.55E-01	2.40E-04	1.86E+16	2.86E+00
74	6	3Pe 1	3Po17	3	3	0.210	59.040	94.20	4427.07	1.42E-02	2.95E-05	2.14E+15	1.15E-01
74	6	3Pe 1	3Po17	5	3	0.215	57.667	191.83	4427.07	2.99E-05	1.06E-07	7.18E+12	2.41E-04
74	6	3Pe 1	3Do17	5	7	0.211	58.760	191.83	4514.27	8.18E-02	2.84E-04	8.76E+15	6.59E-01
74	6	3Pe 1	3So17	1	3	0.202	61.378	0.00	4515.37	3.24E-05	2.16E-08	1.77E+12	2.62E-04
74	6	3Pe 1	3So17	3	3	0.206	60.187	94.20	4515.37	1.50E-01	3.06E-04	2.36E+16	1.21E+00
74	6	3Pe 1	3So17	5	3	0.211	58.760	191.83	4515.37	3.45E-02	1.20E-04	8.64E+15	2.78E-01
74	6	1De 1	1Do17	5	5	0.206	60.187	96.26	4517.19	1.63E-01	5.53E-04	2.56E+16	1.31E+00
74	6	3Pe 1	3Po17	3	1	0.206	60.187	94.20	4517.26	2.91E-02	5.92E-05	1.37E+16	2.35E-01
74	6	1De 1	1Po17	5	3	0.206	60.187	96.26	4518.69	4.55E-02	1.54E-04	1.19E+16	3.67E-01
74	6	1Se 1	1Po17	1	3	0.211	58.760	195.83	4518.69	1.74E-01	1.21E-04	8.70E+15	1.40E+00
74	6	3Pe 1	3Do17	3	5	0.202	61.378	94.20	4605.41	1.23E-07	2.46E-10	1.21E+10	9.93E-07
74	6	3Pe 1	3Do17	5	5	0.206	60.187	191.83	4605.41	9.29E-02	3.16E-04	1.45E+16	7.49E-01
74	6	3Pe 1	3Do17	1	3	0.198	62.618	0.00	4608.21	1.26E-07	8.21E-11	7.17E+09	1.02E-06
74	6	3Pe 1	3Do17	3	3	0.202	61.378	94.20	4608.21	1.98E-05	3.95E-08	3.24E+12	1.60E-04
74	6	3Pe 1	3Do17	5	3	0.206	60.187	191.83	4608.21	8.94E-02	3.03E-04	2.33E+16	7.21E-01
74	6	1De 1	3Po17	5	5	0.21	58.760	96.26	4424.11	3.95E-02	1.37E-04	5.94E+15	3.18E-01
74	6	1De 1	3Po17	5	3	0.21	59.040	96.26	4427.07	4.16E-02	1.44E-04	1.04E+16	3.35E-01
74	6	1Se 1	3Po17	1	3	0.21	57.667	195.83	4427.07	3.77E-05	2.67E-08	1.81E+12	3.04E-04
74	6	3Pe 1	5So17	3	5	0.21	60.187	94.20	4511.02	5.06E-02	1.03E-04	4.76E+15	4.08E-01
74	6	1De 1	5So17	5	5	0.21	60.187	96.26	4511.02	1.97E-03	6.71E-06	3.09E+14	1.59E-02
74	6	3Pe 1	5So17	5	5	0.21	58.760	191.83	4511.02	1.98E-02	6.87E-05	2.96E+15	1.59E-01
74	6	1De 1	3Do17	5	7	0.21	60.187	96.26	4514.27	4.33E-02	1.47E-04	4.85E+15	3.49E-01
74	6	1De 1	3So17	5	3	0.21	60.187	96.26	4515.37	1.88E-02	6.38E-05	4.91E+15	1.52E-01
74	6	1Se 1	3So17	1	3	0.21	58.760	195.83	4515.37	5.15E-08	3.58E-11	2.57E+09	4.15E-07
74	6	3Pe 1	1Do17	3	5	0.21	60.187	94.20	4517.19	2.54E-02	5.17E-05	2.40E+15	2.05E-01
74	6	3Pe 1	1Do17	5	5	0.21	58.760	191.83	4517.19	3.82E-02	1.33E-04	5.75E+15	3.08E-01
74	6	3Pe 1	1Po17	1	3	0.20	61.378	0.00	4518.69	2.31E-05	1.54E-08	1.26E+12	1.87E-04

Table 2 continues

Z	Ne	slpc:i	slpc:j	gi	gj	wl(Å)	E(Kev)	Ei(Ry)	Ej(Ry)	fij	S	Aji(s-1)	σ_{pi}(Mb)
74	6	3Pe 1	1Po17	3	3	0.21	60.187	94.20	4518.69	1.35E-02	2.74E-05	2.12E+15	1.09E-01
74	6	3Pe 1	1Po17	5	3	0.21	58.760	191.83	4518.69	6.89E-06	2.39E-08	1.73E+12	5.56E-05
74	6	1De 1	3Do17	5	5	0.20	61.378	96.26	4605.41	9.50E-06	3.16E-08	1.55E+12	7.66E-05
74	6	1De 1	3Do17	5	3	0.20	61.378	96.26	4608.21	4.99E-08	1.66E-10	1.36E+10	4.03E-07
74	6	1Se 1	3Do17	1	3	0.21	59.896	195.83	4608.21	1.86E-01	1.27E-04	9.71E+15	1.50E+00
LS							4377.30	59.556	138.85	4516.16	4.27E-01	2.63E-03	6.57E+16	3.44E+00
Total:No of trans= 35							Ekev= 59.556			f,CS,Absrp cf=		1.78E+00	1.43E+01	4.70E+04
N-like: C_i(1)=1s1s2s2s2p2p2p , C_j(14)= 1s2s2s2p2p2p2p														
74	7	4So 1	4Pe14	4	6	0.211	58.760	92.69	4409.54	6.79E-02	1.89E-04	6.77E+15	5.47E-01
74	7	2Do 1	2Pe14	4	4	0.206	60.187	0.00	4413.12	1.75E-01	4.76E-04	2.74E+16	1.41E+00
74	7	2Do 1	2Pe14	6	4	0.211	58.760	95.28	4413.12	4.46E-02	1.86E-04	1.00E+16	3.60E-01
74	7	2Po 1	2Pe14	2	4	0.211	58.760	98.18	4413.12	3.34E-06	4.65E-09	2.50E+11	2.70E-05
74	7	2Po 1	2Pe14	4	4	0.216	57.400	191.33	4413.12	4.33E-05	1.23E-07	6.20E+12	3.49E-04
74	7	2Po 1	2Se14	2	2	0.211	58.760	98.18	4414.89	8.31E-02	1.16E-04	1.24E+16	6.70E-01
74	7	2Po 1	2Se14	4	2	0.216	57.400	191.33	4414.89	1.52E-05	4.31E-08	4.35E+12	1.22E-04
74	7	4So 1	4Pe14	4	4	0.207	59.896	92.69	4498.33	8.49E-02	2.31E-04	1.32E+16	6.84E-01
74	7	2Do 1	2De14	4	6	0.202	61.378	0.00	4501.11	2.40E-06	6.39E-09	2.60E+11	1.93E-05
74	7	2Do 1	2De14	6	6	0.207	59.896	95.28	4501.11	8.50E-02	3.47E-04	1.33E+16	6.86E-01
74	7	2Po 1	2De14	4	6	0.211	58.760	191.33	4501.11	8.84E-02	2.46E-04	8.79E+15	7.13E-01
74	7	2Do 1	2Pe14	4	2	0.202	61.378	0.00	4501.89	1.66E-06	4.42E-09	5.40E+11	1.34E-05
74	7	2Po 1	2Pe14	2	2	0.207	59.896	98.18	4501.89	6.30E-02	8.59E-05	9.82E+15	5.08E-01
74	7	2Po 1	2Pe14	4	2	0.211	58.760	191.33	4501.89	2.88E-02	8.01E-05	8.59E+15	2.32E-01
74	7	2Do 1	2De14	4	4	0.202	61.378	0.00	4503.26	1.54E-05	4.10E-08	2.51E+12	1.24E-04
74	7	2Do 1	2De14	6	4	0.207	59.896	95.28	4503.26	9.12E-02	3.72E-04	2.13E+16	7.35E-01
74	7	2Po 1	2De14	2	4	0.207	59.896	98.18	4503.26	1.19E-01	1.63E-04	9.30E+15	9.63E-01
74	7	2Po 1	2De14	4	4	0.211	58.760	191.33	4503.26	4.06E-02	1.13E-04	6.06E+15	3.27E-01
74	7	4So 1	4Pe14	4	2	0.203	61.076	92.69	4592.14	8.43E-06	2.25E-08	2.74E+12	6.79E-05
74	7	2Do 1	4Pe14	4	6	0.21	59.896	0.00	4409.54	4.60E-02	1.25E-04	4.79E+15	3.71E-01
74	7	2Do 1	4Pe14	6	6	0.21	58.760	95.28	4409.54	3.71E-02	1.55E-04	5.55E+15	2.99E-01
74	7	2Po 1	4Pe14	4	6	0.22	57.400	191.33	4409.54	9.37E-06	2.67E-08	8.93E+11	7.55E-05
74	7	4So 1	2Pe14	4	4	0.21	58.760	92.69	4413.12	1.78E-02	4.96E-05	2.68E+15	1.44E-01
74	7	2Do 1	2Se14	4	2	0.21	60.187	0.00	4414.89	4.33E-02	1.18E-04	1.36E+16	3.49E-01
74	7	4So 1	2Se14	4	2	0.21	58.760	92.69	4414.89	2.53E-06	7.03E-09	7.60E+11	2.04E-05
74	7	2Do 1	4Pe14	4	4	0.20	61.076	0.00	4498.33	9.89E-06	2.64E-08	1.61E+12	7.97E-05
74	7	2Do 1	4Pe14	6	4	0.21	59.896	95.28	4498.33	4.61E-03	1.88E-05	1.08E+15	3.71E-02
74	7	2Po 1	4Pe14	2	4	0.21	59.896	98.18	4498.33	2.42E-04	3.30E-07	1.88E+13	1.95E-03
74	7	2Po 1	4Pe14	4	4	0.21	58.483	191.33	4498.33	1.85E-02	5.15E-05	2.75E+15	1.49E-01
74	7	4So 1	2De14	4	6	0.21	59.896	92.69	4501.11	8.36E-03	2.28E-05	8.70E+14	6.74E-02
74	7	4So 1	2Pe14	4	2	0.21	59.896	92.69	4501.89	7.19E-02	1.96E-04	2.25E+16	5.80E-01
74	7	4So 1	2De14	4	4	0.21	59.896	92.69	4503.26	1.08E-02	2.93E-05	1.68E+15	8.67E-02
74	7	2Do 1	4Pe14	4	2	0.20	62.618	0.00	4592.14	3.27E-08	8.54E-11	1.11E+10	2.64E-07
74	7	2Po 1	4Pe14	2	2	0.20	61.076	98.18	4592.14	1.07E-05	1.42E-08	1.73E+12	8.60E-05
74	7	2Po 1	4Pe14	4	2	0.21	59.896	191.33	4592.14	9.08E-02	2.48E-04	2.83E+16	7.32E-01
LS							4371.52	59.478	100.53	4472.05	9.49E-01	2.60E-03	4.85E+16	7.65E+00
Total:No of trans= 35							Ekev= 59.478			f,CS,Absrp cf=		1.32E+00	1.07E+01	3.49E+04
O-like: C_i(1)=1s1s2s2s2p2p2p2p , C_j(18)= 1s2s2s2p2p2p2p2p														
74	8	3Pe 1	3Po18	5	5	0.207	59.896	0.00	4411.16	8.59E-02	2.92E-04	1.34E+16	6.92E-01
74	8	3Pe 1	3Po18	3	5	0.211	58.760	91.66	4411.16	6.89E-02	1.44E-04	6.20E+15	5.56E-01
74	8	1Se 1	1Po18	1	3	0.207	59.896	3.86	4413.86	1.72E-01	1.17E-04	8.94E+15	1.38E+00
74	8	1De 1	1Po18	5	3	0.211	58.760	93.73	4413.86	4.07E-02	1.41E-04	1.02E+16	3.29E-01
74	8	3Pe 1	3Po18	3	1	0.207	59.896	91.66	4497.32	5.63E-02	1.15E-04	2.64E+16	4.54E-01
74	8	3Pe 1	3Po18	5	3	0.203	61.076	0.00	4498.74	6.51E-06	2.17E-08	1.76E+12	5.25E-05
74	8	3Pe 1	3Po18	3	3	0.207	59.896	91.66	4498.74	2.73E-02	5.57E-05	4.25E+15	2.20E-01
74	8	3Pe 1	3Po18	1	3	0.211	58.760	186.88	4498.74	1.71E-01	1.19E-04	8.52E+15	1.38E+00
74	8	1De 1	3Po18	5	5	0.21	58.760	93.73	4411.16	3.95E-02	1.37E-04	5.92E+15	3.19E-01
74	8	3Pe 1	1Po18	5	3	0.21	60.187	0.00	4413.86	8.26E-02	2.81E-04	2.15E+16	6.66E-01
74	8	3Pe 1	1Po18	3	3	0.21	58.760	91.66	4413.86	1.47E-02	3.06E-05	2.20E+15	1.18E-01
74	8	3Pe 1	1Po18	1	3	0.22	57.400	186.88	4413.86	4.99E-05	3.54E-08	2.39E+12	4.03E-04
74	8	1Se 1	3Po18	1	3	0.20	61.076	3.86	4498.74	2.17E-05	1.45E-08	1.17E+12	1.75E-04
74	8	1De 1	3Po18	5	3	0.21	59.896	93.73	4498.74	8.76E-02	2.98E-04	2.28E+16	7.07E-01
LS							4388.32	59.706	57.09	4445.41	1.60E-01	9.84E-04	2.47E+16	1.29E+00
Total:No of trans= 14							Ekev= 59.706			f,CS,Absrp cf=		8.47E-01	6.83E+00	2.24E+04
F-like: C_i(1)=1s1s2s2s2p2p2p2p2p , C_j(16)= 1s2s2s2p2p2p2p2p2p														
74	9	2Po 1	2Se16	4	2	0.207	59.896	0.00	4395.04	8.72E-02	2.38E-04	2.70E+16	7.03E-01
74	9	2Po 1	2Se16	2	2	0.212	58.483	93.83	4395.04	8.56E-02	1.19E-04	1.27E+16	6.90E-01
LS							4363.76	59.372	31.28	4395.04	8.67E-02	3.57E-04	3.98E+16	6.99E-01
Total:No of trans= 2							Ekev= 59.372			f,CS,Absrp cf=		1.73E-01	1.39E+00	4.56E+03
Pb Ions														
H-like: C_i(1)=1s , C_j(3)= 2p														
82	1	2Se 1	2Po 3	2	2	0.166	74.689	0.00	5473.80	9.53E-02	1.04E-04	2.29E+16	7.68E-01
82	1	2Se 1	2Po 3	2	4	0.162	76.533	0.00	5637.52	1.88E-01	2.00E-04	2.40E+16	1.52E+00
LS							5582.95	75.960	0.00	5582.95	2.83E-01	3.04E-04	2.36E+16	2.28E+00
Total:No of trans= 2							Ekev= 75.960			f,CS,Absrp cf=		2.83E-01	2.28E+00	6.64E+03
He-like: C_i(1)=1s1s , C_j(3)= 1s2p														
82	2	1Se 1	1Po 3	1	3	0.164	75.600	0.00	5564.56	3.80E-01	2.05E-04	3.15E+16	3.06E+00
82	2	1Se 1	3Po 3	1	3	0.17	73.363	0.00	5404.28	1.80E-01	1.00E-04	1.41E+16	1.45E+00
LS							5564.56	75.710	0.00	5564.56	3.80E-01	2.05E-04	3.15E+16	3.06E+00
Total:No of trans= 2							Ekev= 75.710			f,CS,Absrp cf=		5.60E-01	4.52E+00	1.31E+04

Table 2 continues

Z	Ne	slpc:i	slpc:j	gi	gj	wl(Å)	E(Kev)	Ei(Ry)	Ej(Ry)	fij	S	Aji(s-1)	σ_{ij}(Mb)
Li-like: $C_i(1)$=1s1s2s , $C_j(11)$= 1s2s2p													
82	3	2Se 1	2Po11	2	2	0.167	74.242	0.00	5461.71	4.84E-02	5.32E-05	1.16E+16	3.90E-01
82	3	2Se 1	2Po11	2	4	0.164	75.600	0.00	5559.44	1.67E-01	1.81E-04	2.08E+16	1.35E+00
82	3	2Se 1	2Po11	2	2	0.164	75.600	0.00	5563.29	1.19E-01	1.28E-04	2.96E+16	9.59E-01
82	3	2Se 1	2Po11	2	4	0.162	76.533	0.00	5614.98	8.25E-02	8.82E-05	1.04E+16	6.66E-01
82	3	2Se 1	4Po11	2	2	0.17	73.363	0.00	5400.89	1.38E-02	1.53E-05	3.23E+15	1.11E-01
82	3	2Se 1	4Po11	2	4	0.17	73.363	0.00	5404.75	1.13E-01	1.25E-04	1.32E+16	9.07E-01
LS						5562.31	75.679	0.00	5562.31	4.17E-01	4.50E-04	3.46E+16	3.37E+00
Total:No of trans= 6						Ekev= 75.679			f,CS,Absrp cf=		5.44E-01	4.38E+00	1.27E+04
Be-like: $C_i(1)$=1s1s2s2s , $C_j(28)$= 1s2s2s2p													
82	4	1Se 1	1Po28	1	3	0.164	75.600	1.68	5569.31	3.28E-01	1.77E-04	2.72E+16	2.64E+00
82	4	1Se 1	3Po28	1	3	0.17	73.800	1.68	5429.30	1.57E-01	8.68E-05	1.24E+16	1.27E+00
LS						5567.62	75.751	1.68	5569.31	3.28E-01	1.77E-04	2.72E+16	2.64E+00
Total:No of trans= 2						Ekev= 75.751			f,CS,Absrp cf=		4.85E-01	3.91E+00	1.14E+04
B-like: $C_i(1)$=1s1s2s2s2p , $C_j(22)$= 1s2s2s2p2p													
82	5	2Po 1	2De22	2	4	0.164	75.600	0.00	5552.01	4.62E-04	5.00E-07	5.72E+13	3.73E-03
82	5	2Po 1	2De22	4	4	0.169	73.363	147.67	5552.01	1.90E-02	4.22E-05	4.46E+15	1.53E-01
82	5	2Po 1	2De22	4	6	0.169	73.363	147.67	5555.26	9.06E-02	2.01E-04	1.42E+16	7.31E-01
82	5	2Po 1	2Pe22	2	2	0.164	75.600	0.00	5556.27	1.18E-01	1.27E-04	2.92E+16	9.50E-01
82	5	2Po 1	2Pe22	4	2	0.168	73.800	147.67	5556.27	3.02E-02	6.70E-05	1.42E+16	2.44E-01
82	5	2Po 1	2Pe22	2	4	0.160	77.490	0.00	5703.30	8.80E-06	9.26E-09	1.15E+12	7.10E-05
82	5	2Po 1	2Pe22	4	4	0.164	75.600	147.67	5703.30	1.71E-01	3.70E-04	4.25E+16	1.38E+00
82	5	2Po 1	2Se22	2	2	0.160	77.490	0.00	5705.47	9.37E-06	9.85E-09	2.45E+12	7.56E-05
82	5	2Po 1	2Se22	4	2	0.164	75.600	147.67	5705.47	4.20E-02	9.08E-05	2.09E+16	3.39E-01
82	5	2Po 1	4Pe22	2	2	0.17	73.800	0.00	5410.92	8.42E-02	9.33E-05	1.98E+16	6.79E-01
82	5	2Po 1	4Pe22	4	2	0.17	71.667	147.67	5410.92	9.34E-05	2.13E-07	4.16E+13	7.53E-04
82	5	2Po 1	4Pe22	2	4	0.16	75.600	0.00	5557.78	2.26E-01	2.44E-04	2.81E+16	1.82E+00
82	5	2Po 1	4Pe22	4	4	0.17	73.800	147.67	5557.78	4.08E-02	9.05E-05	9.59E+15	3.29E-01
82	5	2Po 1	4Pe22	4	6	0.16	75.600	147.67	5699.25	4.45E-02	9.62E-05	7.34E+15	3.59E-01
LS						5508.55	74.948	105.48	5614.03	2.75E-01	8.99E-04	4.02E+16	2.22E+00
Total:No of trans= 14						Ekev= 74.948			f,CS,Absrp cf=		8.67E-01	6.99E+00	2.03E+04
C-like: $C_i(1)$=1s1s2s2s2p2p , $C_j(17)$= 1s2s2s2p2p2p													
82	6	3Pe 1	3Po17	3	5	0.168	73.800	145.97	5570.28	6.36E-02	1.06E-04	9.02E+15	5.13E-01
82	6	3Pe 1	3Po17	5	5	0.173	71.667	295.99	5570.28	3.15E-05	8.96E-08	7.04E+12	2.54E-04
82	6	3Pe 1	3Po17	1	3	0.163	76.064	0.00	5573.50	3.22E-01	1.73E-04	2.68E+16	2.60E+00
82	6	3Pe 1	3Po17	3	3	0.168	73.800	145.97	5573.50	1.29E-02	2.15E-05	3.06E+15	1.04E-01
82	6	3Pe 1	3Po17	5	3	0.173	71.667	295.99	5573.50	3.42E-05	9.71E-08	1.27E+13	2.76E-04
82	6	3Pe 1	3Do17	5	7	0.168	73.800	295.99	5707.63	7.48E-02	2.07E-04	1.26E+16	6.03E-01
82	6	3Pe 1	3So17	1	3	0.160	77.490	0.00	5708.80	1.60E-05	8.43E-09	1.40E+12	1.29E-04
82	6	3Pe 1	3So17	3	3	0.164	75.600	145.97	5708.80	1.36E-01	2.20E-04	3.39E+16	1.10E+00
82	6	3Pe 1	3So17	5	3	0.168	73.800	295.99	5708.80	3.18E-02	8.82E-05	1.25E+16	2.57E-01
82	6	1De 1	1Do17	5	5	0.164	75.600	148.29	5710.84	1.48E-01	3.99E-04	3.68E+16	1.19E+00
82	6	3Pe 1	3Po17	3	1	0.164	75.600	145.97	5710.95	2.65E-02	4.28E-05	1.98E+16	2.13E-01
82	6	1De 1	1Po17	5	3	0.164	75.600	148.29	5712.53	4.10E-02	1.10E-04	1.70E+16	3.30E-01
82	6	1Se 1	1Po17	1	3	0.168	73.800	300.48	5712.53	1.60E-01	8.85E-05	1.25E+16	1.29E+00
82	6	3Pe 1	3Do17	3	5	0.160	77.490	145.97	5846.08	2.89E-07	4.57E-10	4.53E+10	2.33E-06
82	6	3Pe 1	3Do17	5	5	0.164	75.600	295.99	5846.08	8.35E-02	2.26E-04	2.07E+16	6.74E-01
82	6	3Pe 1	3Do17	1	3	0.156	79.477	0.00	5849.18	4.95E-08	2.54E-11	4.53E+09	3.99E-07
82	6	3Pe 1	3Do17	3	3	0.160	77.490	145.97	5849.18	1.08E-05	1.71E-08	2.83E+12	8.72E-05
82	6	3Pe 1	3Do17	5	3	0.164	75.600	295.99	5849.18	8.13E-02	2.20E-04	3.36E+16	6.56E-01
82	6	1De 1	3Po17	5	5	0.17	73.800	148.29	5570.28	3.66E-02	1.01E-04	8.64E+15	2.95E-01
82	6	1De 1	3Po17	5	3	0.17	73.800	148.29	5573.50	3.80E-02	1.05E-04	1.50E+16	3.07E-01
82	6	1Se 1	3Po17	1	3	0.17	71.667	300.48	5573.50	5.22E-05	2.97E-08	3.89E+12	4.21E-04
82	6	3Pe 1	5So17	3	5	0.16	75.600	145.97	5704.02	4.49E-02	7.28E-05	6.69E+15	3.62E-01
82	6	1De 1	5So17	5	5	0.16	75.600	148.29	5704.02	1.75E-03	4.73E-06	4.34E+14	1.41E-02
82	6	3Pe 1	5So17	5	5	0.17	73.363	295.99	5704.02	1.85E-02	5.14E-05	4.36E+15	1.50E-01
82	6	1De 1	3Do17	5	7	0.16	75.600	148.29	5707.63	3.89E-02	1.05E-04	6.90E+15	3.14E-01
82	6	1De 1	3So17	5	3	0.16	75.600	148.29	5708.80	1.69E-02	4.55E-05	6.98E+15	1.36E-01
82	6	1Se 1	3So17	1	3	0.17	73.800	300.48	5708.80	7.26E-08	4.03E-11	5.69E+09	5.86E-07
82	6	3Pe 1	1Do17	3	5	0.16	75.600	145.97	5710.84	2.36E-02	3.82E-05	3.52E+15	1.90E-01
82	6	3Pe 1	1Do17	5	5	0.17	73.800	295.99	5710.84	3.47E-02	9.61E-05	8.17E+15	2.80E-01
82	6	3Pe 1	1Po17	1	3	0.16	77.490	0.00	5712.53	1.54E-05	8.09E-09	1.35E+12	1.24E-04
82	6	3Pe 1	1Po17	3	3	0.16	75.600	145.97	5712.53	1.26E-02	2.03E-05	3.12E+15	1.01E-01
82	6	3Pe 1	1Po17	5	3	0.17	73.800	295.99	5712.53	2.80E-06	7.76E-09	1.10E+12	2.26E-05
82	6	1De 1	3Do17	5	5	0.16	77.490	148.29	5846.08	5.73E-06	1.51E-08	1.49E+12	4.62E-05
82	6	1De 1	3Do17	5	3	0.16	77.490	148.29	5849.18	1.21E-07	3.18E-10	5.26E+10	9.75E-07
82	6	1Se 1	3Do17	1	3	0.16	75.600	300.48	5849.18	1.68E-01	9.10E-05	1.39E+16	1.36E+00
LS						5495.35	74.768	214.36	5709.71	3.87E-01	1.90E-03	9.39E+16	3.12E+00
Total:No of trans= 35						Ekev= 74.768			f,CS,Absrp cf=		1.62E+00	1.30E+01	3.79E+04
N-like: $C_i(1)$=1s1s2s2s2p2p2p , $C_j(14)$= 1s2s2s2p2p2p2p													
82	7	4So 1	4Pe14	4	6	0.169	73.363	144.05	5551.02	6.16E-02	1.37E-04	9.64E+15	4.97E-01
82	7	2Do 1	2Pe14	4	4	0.164	75.600	0.00	5554.96	1.59E-01	3.44E-04	3.95E+16	1.28E+00
82	7	2Do 1	2Pe14	6	4	0.169	73.363	146.95	5554.96	4.08E-02	1.36E-04	1.44E+16	3.29E-01
82	7	2Po 1	2Pe14	2	4	0.169	73.363	150.22	5554.96	1.24E-06	1.38E-09	1.46E+11	1.00E-05
82	7	2Po 1	2Pe14	4	4	0.173	71.667	294.95	5554.96	5.83E-05	1.33E-07	1.30E+13	4.70E-04
82	7	2Po 1	2Se14	2	2	0.169	73.363	150.22	5556.97	7.60E-02	8.43E-05	1.78E+16	6.13E-01
82	7	2Po 1	2Se14	4	2	0.173	71.667	294.95	5556.97	1.77E-05	4.04E-08	7.88E+12	1.43E-04

Table 2 continues

Z	Ne	slpc:i	slpc:j	gi	gj	wl(Å)	E(Kev)	Ei(Ry)	Ej(Ry)	fij	S	Aji(s-1)	$\sigma_{I'I}$(Mb)
82	7	2Do 1	2De14	4	4	0.160	77.490	0.00	5686.67	5.45E-06	1.15E-08	1.42E+12	4.39E-05
82	7	2Do 1	2De14	6	4	0.164	75.600	146.95	5686.67	4.11E-03	1.34E-05	1.52E+15	3.32E-02
82	7	2Po 1	2De14	2	4	0.165	75.142	150.22	5686.67	1.98E-04	2.14E-07	2.44E+13	1.60E-03
82	7	2Po 1	2De14	4	4	0.169	73.363	294.95	5686.67	1.72E-02	3.84E-05	4.03E+15	1.39E-01
82	7	2Do 1	2De14	4	6	0.160	77.490	0.00	5689.75	1.91E-06	4.03E-09	3.31E+11	1.54E-05
82	7	2Do 1	2De14	6	6	0.164	75.600	146.95	5689.75	7.66E-02	2.49E-04	1.89E+16	6.18E-01
82	7	2Po 1	2De14	4	6	0.169	73.363	294.95	5689.75	8.07E-02	1.80E-04	1.26E+16	6.51E-01
82	7	2Do 1	2Pe14	4	2	0.160	77.490	0.00	5690.61	5.86E-07	1.23E-09	3.05E+11	4.72E-06
82	7	2Po 1	2Pe14	2	2	0.164	75.600	150.22	5690.61	5.65E-02	6.11E-05	1.39E+16	4.55E-01
82	7	2Po 1	2Pe14	4	2	0.169	73.363	294.95	5690.61	2.65E-02	5.90E-05	1.24E+16	2.14E-01
82	7	4So 1	4Pe14	4	4	0.164	75.600	144.05	5692.13	1.01E-02	2.19E-05	2.50E+15	8.17E-02
82	7	4So 1	4Pe14	4	2	0.160	77.490	144.05	5827.89	4.33E-06	9.15E-09	2.25E+12	3.49E-05
82	7	2Do 1	4Pe14	4	6	0.16	75.600	0.00	5551.02	4.12E-02	8.91E-05	6.80E+15	3.33E-01
82	7	2Do 1	4Pe14	6	6	0.17	73.363	146.95	5551.02	3.43E-02	1.14E-04	8.04E+15	2.77E-01
82	7	2Po 1	4Pe14	4	6	0.17	71.667	294.95	5551.02	1.32E-05	3.01E-08	1.95E+12	1.06E-04
82	7	4So 1	2Pe14	4	4	0.17	73.800	144.05	5554.96	1.60E-02	3.55E-05	3.76E+15	1.29E-01
82	7	2Do 1	2Se14	4	2	0.16	75.600	0.00	5556.97	3.94E-02	8.50E-05	1.95E+16	3.17E-01
82	7	4So 1	2Se14	4	2	0.17	73.800	144.05	5556.97	9.58E-07	2.12E-09	4.51E+11	7.72E-06
82	7	4So 1	2De14	4	4	0.16	75.600	144.05	5686.67	7.63E-02	1.65E-04	1.88E+16	6.15E-01
82	7	4So 1	2De14	4	6	0.16	75.600	144.05	5689.75	7.71E-03	1.67E-05	1.27E+15	6.21E-02
82	7	4So 1	2Pe14	4	2	0.16	75.600	144.05	5690.61	6.58E-02	1.42E-04	3.25E+16	5.31E-01
82	7	2Do 1	4Pe14	4	4	0.16	77.490	0.00	5692.13	8.65E-06	1.82E-08	2.25E+12	6.98E-05
82	7	2Do 1	4Pe14	6	4	0.16	75.600	146.95	5692.13	8.25E-02	2.68E-04	3.06E+16	6.66E-01
82	7	2Po 1	4Pe14	2	4	0.16	75.600	150.22	5692.13	1.08E-01	1.17E-04	1.34E+16	8.75E-01
82	7	2Po 1	4Pe14	4	4	0.17	73.363	294.95	5692.13	3.67E-02	8.16E-05	8.58E+15	2.96E-01
82	7	2Do 1	4Pe14	4	2	0.16	79.477	0.00	5827.89	1.26E-08	2.59E-11	6.86E+09	1.01E-07
82	7	2Po 1	4Pe14	2	2	0.16	77.009	150.22	5827.89	7.52E-06	7.95E-09	1.95E+12	6.07E-05
82	7	2Po 1	4Pe14	4	2	0.17	75.142	294.95	5827.89	8.22E-02	1.78E-04	4.04E+16	6.62E-01
LS						5489.16	74.684	155.06	5644.22	6.05E-01	1.32E-03	4.88E+16	4.88E+00
Total:No of trans= 35						Ekev= 74.684			f,CS,Absrp cf=		1.20E+00	9.68E+00	2.81E+04
O-like: C_i(1)=1s1s2s2s2p2p2p2p , C_j(18)= 1s2s2s2p2p2p2p2p													
82	8	3Pe 1	3Po18	5	5	0.164	75.600	0.00	5555.86	7.76E-02	2.10E-04	1.92E+16	6.26E-01
82	8	3Pe 1	3Po18	3	5	0.168	73.800	142.02	5555.86	6.24E-02	1.04E-04	8.81E+15	5.03E-01
82	8	1Se 1	1Po18	1	3	0.164	75.600	4.36	5558.85	1.56E-01	8.42E-05	1.29E+16	1.26E+00
82	8	1De 1	1Po18	5	3	0.168	73.800	144.34	5558.85	3.72E-02	1.03E-04	1.46E+16	3.00E-01
82	8	3Pe 1	3Po18	3	1	0.164	75.600	142.02	5687.70	5.13E-02	8.33E-05	3.80E+16	4.14E-01
82	8	3Pe 1	3Po18	5	3	0.160	77.490	0.00	5689.25	3.30E-06	8.71E-09	1.43E+12	2.67E-05
82	8	3Pe 1	3Po18	3	3	0.164	75.600	142.02	5689.25	2.51E-02	4.07E-05	6.20E+15	2.02E-01
82	8	3Pe 1	3Po18	1	3	0.169	73.363	288.20	5689.25	1.56E-01	8.66E-05	1.22E+16	1.26E+00
82	8	1De 1	3Po18	5	5	0.17	73.800	144.34	5555.86	3.63E-02	1.00E-04	8.53E+15	2.92E-01
82	8	3Pe 1	1Po18	5	3	0.16	75.600	0.00	5558.85	7.56E-02	2.04E-04	3.13E+16	6.09E-01
82	8	3Pe 1	1Po18	3	3	0.17	73.800	142.02	5558.85	1.31E-02	2.17E-05	3.08E+15	1.05E-01
82	8	3Pe 1	1Po18	1	3	0.17	71.667	288.20	5558.85	6.51E-05	3.70E-08	4.84E+12	5.25E-04
82	8	1Se 1	3Po18	1	3	0.16	77.490	4.36	5689.25	1.44E-05	7.61E-09	1.25E+12	1.16E-04
82	8	1De 1	3Po18	5	3	0.16	75.600	144.34	5689.25	7.91E-02	2.14E-04	3.25E+16	6.38E-01
LS						5519.63	75.098	88.17	5607.80	1.45E-01	7.11E-04	3.56E+16	1.17E+00
Total:No of trans= 14						Ekev= 75.098			f,CS,Absrp cf=		7.69E-01	6.20E+00	1.80E+04
F-like: C_i(1)=1s1s2s2s2p2p2p2p2p , C_j(16)= 1s2s2s2p2p2p2p2p													
82	9	2Po 1	2Se16	4	2	0.165	75.325	0.00	5536.66	7.92E-02	1.72E-04	3.90E+16	6.39E-01
82	9	2Po 1	2Se16	2	2	0.169	73.363	144.81	5536.66	7.75E-02	8.62E-05	1.81E+16	6.25E-01
LS						5488.39	74.673	48.27	5536.66	7.86E-02	2.58E-04	5.71E+16	6.34E-01
Total:No of trans= 2						Ekev= 74.673			f,CS,Absrp cf=		1.57E-01	1.26E+00	3.67E+03